

## Thermal QCD with external imaginary electric fields on the lattice

---

**Gergely Endródi<sup>a,\*</sup> and Gergely Markó<sup>a</sup>**

<sup>a</sup>*Fakultät für Physik, Universität Bielefeld  
D-33615 Bielefeld, Germany.*

*E-mail:* [endrodi@physik.uni-bielefeld.de](mailto:endrodi@physik.uni-bielefeld.de), [gmarko@physik.uni-bielefeld.de](mailto:gmarko@physik.uni-bielefeld.de)

We study QCD at finite temperature in the presence of imaginary electric fields. In particular, we determine the electric susceptibility, the leading coefficient in the expansion of the QCD pressure in the imaginary field. Unlike for magnetic fields, at nonzero temperature this coefficient requires a non-trivial separation of genuine electric field-related effects and spurious effects related to the chemical potential, which becomes an unphysical gauge parameter in this setting. Our results are based on lattice simulations with stout improved dynamical staggered quarks at physical quark masses.

*The 38th International Symposium on Lattice Field Theory, LATTICE2021 26th-30th July, 2021  
Zoom/Gather@Massachusetts Institute of Technology*

---

\*Speaker

## 1. Introduction

It is by now well established that the early stages of off-central heavy-ion collisions exhibit strong electromagnetic fields [1], even if only for a short period of time [2, 3]. The magnetic components received most attention due to their possible phenomenological impact via, e.g., the chiral magnetic effect [4]. On an event-by-event basis, the electric components can however be as large as the magnetic ones, reaching up to values  $\propto O(m_\pi^2)$  [5, 6] and therefore affecting strong interaction processes in a potentially significant way. Electric fields are expected to be particularly relevant for asymmetric systems (e.g. copper on gold at RHIC) [7].

In this talk we do not attempt to describe the highly complex out-of-equilibrium system including time-dependent electromagnetic fields. Our focus lies in the treatment of equilibrium strongly interacting matter in the presence of static, homogeneous background fields at nonzero temperature on the lattice. For background *magnetic* fields  $B$  the most important aspects, like the phase diagram [8–10] and the equation of state [11, 12] have already been investigated in detail. For external *electric* fields  $E$  our knowledge is mostly limited to low-temperature effects like electric polarizabilities of hadrons, see, e.g., Refs. [13, 14]. One lattice study discussed charge separation in an unphysical system with isospin electric charges for quarks both at low and at high temperature [15]. Further thermodynamic aspects have been studied perturbatively at high temperature, see e.g. [16].

In comparison to the magnetic case, lattice simulations involving external electric fields entail several new conceptual challenges. First, a constant electric field accelerates charged particles, bringing the system inevitably out of equilibrium, naively inaccessible for standard simulations. Second, as we will see below, at nonzero temperature electric fields automatically enforce an averaging over the chemical potential  $\mu$ , implying a mixing between  $E$  and  $\mu$ . Third, the QCD action becomes complex in the presence of a real electric field, hindering importance sampling-based simulations. Here we aim to solve the first two of these issues and develop an approach that enables an equilibrium discussion and also eliminates the mixing between  $E$  and  $\mu$ . We also discuss a Taylor-expansion method in imaginary electric fields in order to address the complex action problem, but we will not perform an analytic continuation to real electric fields here.

## 2. Equilibrium and mixing with the chemical potential

Instead of a homogeneous electric field, let us consider an oscillatory field of the form  $\mathbf{E}(x_1) = E \cos(p_1 x_1) \mathbf{e}_1$ , pointing in the  $x_1$  direction and modulated with a wavelength  $1/p_1$ , see Fig. 1. In this setting, the electrically charged particles will move around until the effect of the electric field is balanced by the interactions between them – i.e. the strong force as well as the electromagnetic repulsion (although in this contribution we do not take dynamical QED effects into account). Thus, an equilibrium will be reached and lattice simulations of this setup will correspond to this equilibrium and fluctuations around it. The resulting modulated distribution of the electric charge density (see also Fig. 1) arises due to electric polarization and is described by the electric permittivity of the QCD medium. Once we have approached the infinite volume limit, we can extrapolate the momentum  $p_1$  to zero. For QCD in the absence of dynamical QED effects, interactions fall off exponentially with the distance and the  $p_1 \rightarrow 0$  limit is expected to be smooth already on sufficiently

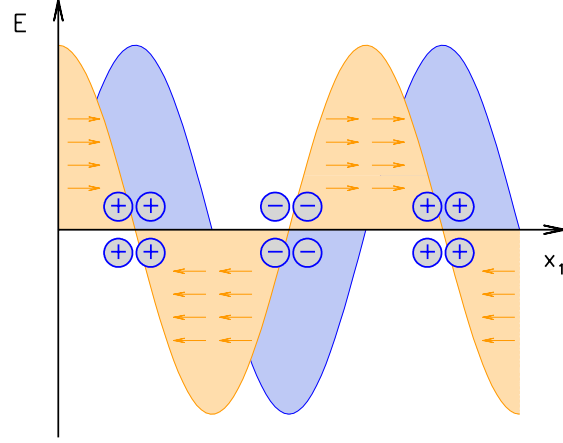


**Figure 1:** Illustration of the equilibrium situation in the presence of an electric field  $E \parallel x_1$  modulated in the  $x_1$  direction (dark yellow area and arrows). Positive (negative) electric charges accumulate at points with  $E = 0$  pointed towards (away from) the electric field, giving rise to the charge density profile indicated by the blue region.

large volumes – we get back to this point below. With this approach we can therefore investigate the impact of constant electric fields via a smooth limit of equilibrium lattice simulations.

To quantify the electric polarization effect, we need to compare the equilibria at  $E = 0$  and at a small but nonzero  $E \neq 0$ . This leads us to the second issue – the mixing of the effect of the electric field and that of the chemical potential at nonzero temperature  $T$ . Here we consider a constant electric field (referring to the above discussion, one may think of a modulated field with long wavelength and zooming into the vicinity of the origin). To avoid time-dependent electromagnetic potentials, we consider the static gauge  $A_0 = Ex_1$  for the electric field. Now on the one hand, at  $E = 0$  the free energy density  $f = -T/V \cdot \log \mathcal{Z}$  depends on  $\mu$ . On the other hand, for  $E \neq 0$  the chemical potential becomes a mere gauge degree of freedom, since the potentials  $A_0 = Ex_1$  and  $A_0 = Ex_1 + \mu$  only differ by an electromagnetic gauge transformation. We are lead to conclude that  $f$ , being a gauge invariant quantity, cannot depend on  $\mu$ . In other words, at  $E \neq 0$  the chemical potential is averaged over automatically. To meaningfully compare the free energies at  $E \neq 0$  and at  $E = 0$ , we therefore have to average over the chemical potentials also for the latter case.

The same effect also arises for imaginary (or, Euclidean) electric fields  $\hat{E}$ , considered in the gauge  $A_4 = \hat{E}x_1$ , and imaginary chemical potentials  $\hat{\mu}$  (from here on we will only work with Euclidean parameters, denoted by the hat). We demonstrate this by calculating the free energy density on the lattice for imaginary electric fields. The latter enter the Dirac operator for a quark with flavor  $q$  via U(1) links  $u_\nu$  in the  $x_1 - x_4$  plane, of the form [17]

$$u_4(n) = e^{ia^2q\hat{E}n_1}, \quad u_1(n)|_{n_1=N_1-1} = e^{-ia^2q\hat{E}N_1n_4}, \quad u_\nu(n) = 1 \quad \text{otherwise}, \quad (1)$$

where  $a$  is the lattice spacing and  $n_\nu = 0 \dots N_\nu - 1$  label the sites of the lattice. For periodic boundary conditions, the electric field is quantized as [18]

$$a^2q\hat{E} = \frac{2\pi N_E}{N_1N_4}, \quad N_E \in \mathbb{Z}. \quad (2)$$

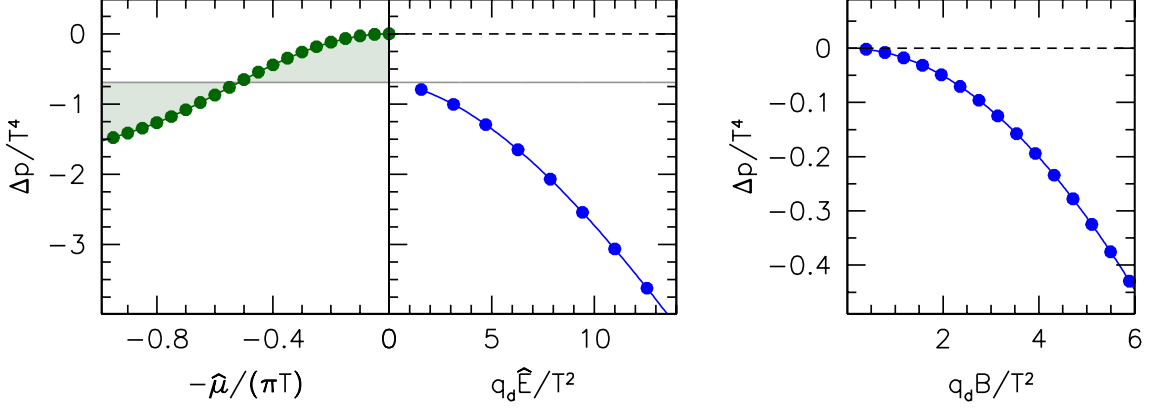


**Figure 2:** The change of the pressure in units of  $T^4$  due to the imaginary chemical potential (left panel), the imaginary electric field (middle panel) and the magnetic field (right panel) in the free case at high temperature. The measurements at quantized fields (blue dots) are connected merely to guide the eye. The measurements at  $i\mu \neq 0$  (green dots) are averaged over all chemical potentials (gray line).

The linear size and the temperature are given by  $L = N_1 a$  and  $T = (N_4 a)^{-1}$ . The quark charges  $q_f$  will be measured in units of the elementary electric charge  $e$ .

For the moment we neglect gluonic interactions so that we may calculate the free energy density by direct diagonalization of the Dirac operator for a colorless fermion. We employ the staggered discretization on a  $24^3 \times 6$  lattice with  $m/T = 0.08$ . The results for the change of the pressure,  $\Delta p = -f + f(\hat{E} = 0, \hat{\mu} = 0)$ , are shown in the middle panel of Fig. 2. Notice the mismatch between the direct evaluation at  $\hat{E} = 0$  (i.e.  $\Delta p = 0$  there) and the continuation  $\hat{E} \rightarrow 0$  using the data at  $\hat{E} > 0$  (pointing clearly to  $\Delta p < 0$ ). As we have seen above, the correct  $\hat{E} = 0$  value is the one obtained by averaging over all imaginary chemical potentials  $0 < \hat{\mu} < \pi T$ , shown in the left panel of the figure.<sup>1</sup> The average of  $\Delta p$  can now be compared meaningfully to the  $\hat{E} > 0$  results. Note that for magnetic fields no such mismatch is observed and the  $B \rightarrow 0$  results extrapolate back to  $\Delta p = 0$ .

The possible values of the imaginary electric field become dense in the thermodynamic limit; in particular the minimal electric field  $q\hat{E}_{\min} = 2\pi T/L$  approaches zero. This implies that for the susceptibility with respect to the imaginary electric field, to be defined below in (5), the mismatch term gives rise to an infrared divergence  $\propto T^4/\hat{E}_{\min}^2 \propto (LT)^2$ .

### 3. Taylor expansion

In the calculations that follow a central role will be played by the electromagnetic current-current correlator (written down before the path integral for quarks is carried out),

$$G_{\mu\nu}(x_1) = \int dx_2 dx_3 dx_4 \langle j_\mu(x) j_\nu(0) \rangle, \quad j_\mu = \bar{\psi} \gamma_\mu \psi. \quad (3)$$

<sup>1</sup>Note that here we discuss the free (colorless) case so no Roberge-Weiss-type transitions are present. The  $2\pi T$  periodicity and the evenness of  $\Delta p$  in  $\hat{\mu}$  imply that the relevant interval is  $0 < \hat{\mu} < \pi T$ , plotted in the figure. Also note that averaging over  $\hat{\mu}$  amounts to considering the expansion of the grand canonical  $\Delta p(\hat{\mu})$  in the fugacity variable  $e^{i\hat{\mu}N/T}$  and projecting to the  $N = 0$  sector.

Since the imaginary chemical potential multiplies  $i$  times the integral of  $j_4$  in the action, the (dimensionless) quark number susceptibility can be calculated in terms of the correlator as

$$c_2 \equiv \frac{1}{T^2} \cdot \frac{T}{V} \left. \frac{\partial^2 \log \mathcal{Z}}{\partial \hat{\mu}^2} \right|_{\hat{\mu}=0} = -\frac{1}{TV} \int d^4x d^4y \langle j_4(x) j_4(y) \rangle = -\frac{1}{T^2} \int dx_1 G_{44}(x_1), \quad (4)$$

where we exploited the translational invariance of the expectation value. (Note that  $c_2 < 0$  for this definition.)

For our periodic boundary conditions, we cannot differentiate with respect to  $\hat{E}$  due to the quantization (2). Let us for the moment switch to open boundary conditions in the  $x_1$  direction (and choose our coordinate system so that  $-L/2 \leq x_1 < L/2$ ). Then we are allowed to repeat the above derivation. The imaginary electric field multiplies  $ie$  times the integral of  $j_4 \cdot x_1$  in the action, so that the susceptibility in this setup (denoted by the bar) reads

$$\bar{\xi} \equiv \frac{T}{V} \left. \frac{\partial^2 \log \mathcal{Z}}{\partial (e\hat{E})^2} \right|_{\hat{E}=0} = -\frac{T}{V} \int d^4x d^4y x_1 y_1 \langle j_4(x) j_4(y) \rangle = -\frac{1}{L} \int dx_1 dy_1 x_1 y_1 G_{44}(x_1 - y_1). \quad (5)$$

Replacing  $x_1 y_1 = (x_1^2 + y_1^2)/2 - (x_1 - y_1)^2/2$ , exploiting again the translational (and this time also parity) invariance of the correlator and denoting  $z_1 = x_1 - y_1$ , we arrive at

$$\bar{\xi} = -\frac{1}{L} \int dx_1 x_1^2 \int dz_1 G_{44}(z_1) + \frac{1}{L} \int dx_1 \int dz_1 \frac{z_1^2}{2} G_{44}(z_1) = \frac{c_2}{12} (LT)^2 + \int dz_1 \frac{z_1^2}{2} G_{44}(z_1), \quad (6)$$

where we recognize the infrared divergent mismatch term  $\propto (LT)^2$  that we anticipated above.

How to extract the physical part of  $\bar{\xi}$ ? To answer this question we again need to consider oscillatory field profiles. For these, the Taylor-expansion in the amplitude of the field – being a continuous variable – is well-defined even for periodic volumes. Moreover, we can extrapolate to constant fields after the thermodynamic limit has been taken. For this, large volumes are already expected to be sufficient, see the discussion regarding equilibrium in Sec. 2. Recently we applied this method for magnetic fields in Ref. [12]. For the magnetic susceptibility, in the  $A_2 = Bx_1$  gauge, the result reads

$$\chi \equiv \frac{T}{V} \left. \frac{\partial^2 \log \mathcal{Z}}{\partial (eB)^2} \right|_{B=0} = \int_0^{L/2} dz_1 z_1^2 G_{22}(z_1). \quad (7)$$

The observable (7) may be recognized as the scalar vacuum polarization that enters the calculation of the muon anomalous magnetic moment [19] – only here we need to calculate it at nonzero temperature. (For alternative methods to determine  $\chi$ , see for example [11, 20].) The calculation for imaginary electric fields is completely analogous, except that this time  $A_4 = \hat{E}x_1$  and therefore the density-density correlator appears,

$$\xi = \int_0^{L/2} dz_1 z_1^2 G_{44}(z_1) = \bar{\xi} - \frac{c_2}{12} (LT)^2, \quad (8)$$

which is just the second term in our naive calculation in (6). This is the physical contribution to the electric susceptibility. Note that the correlators  $G_{\mu\nu}$  fall off exponentially with the distance, which suppresses finite volume effects in (7) and (8), see [12] for more details.

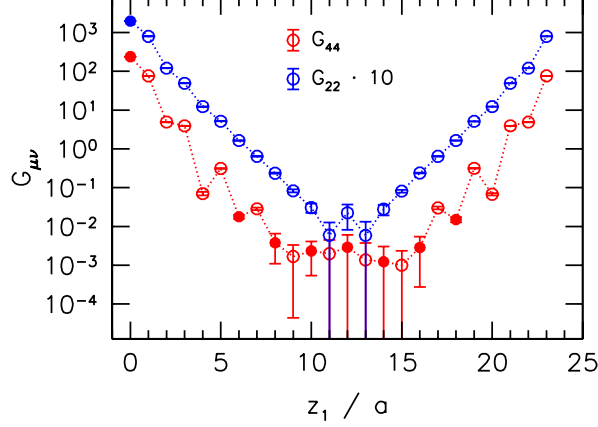


**Figure 3:** Current-current  $G_{22}$  (blue) and density-density  $G_{44}$  (red) correlators at  $T \approx 176$  MeV on our  $N_t = 6$  lattices. The former has been multiplied by a factor of 10 for better visibility. Filled (open) points indicate positive (negative) values.

#### 4. Results

We use the tree-level improved Symanzik gauge action and three flavors of stout smeared staggered quarks with physical masses. The current-current and density-density correlators (3) were determined on  $24^3 \times 6$  lattices for a range of temperatures. We calculated both the connected and the disconnected contributions to  $G_{\mu\nu}$ . To obtain precise results we used up to a thousand noisy estimators, localized to three-dimensional  $x_1$ -slices. For the details of the measured operators, see Ref. [19]. In Fig. 3 we plot the correlators at  $T \approx 176$  MeV, where the difference between the spatial and temporal components is already considerable.

To calculate the susceptibilities (7) and (8) the correlators are convoluted with the quadratic kernel. The results are plotted in the left panel of Fig. 4 for several temperatures. These observables contain an additive divergence in the lattice cutoff (similar to the scalar vacuum polarization that enters the determination of the muon anomalous magnetic moment). To perform the additive renormalization we subtract the value of the bare susceptibilities evaluated at the same lattice spacing but on a  $T \approx 0$  ensemble (note that at  $T = 0$  the magnetic and electric susceptibilities are equal due to Lorentz symmetry). For this we employ the results of Refs. [11, 12]. This defines the renormalized susceptibilities

$$\chi^r = \chi(T) - \chi(T = 0), \quad \xi^r = \xi(T) - \xi(T = 0), \quad (9)$$

which are plotted in the right panel of Fig. 4. The renormalized magnetic susceptibility has been determined in this manner for a set of lattice spacings and a continuum extrapolation was performed in Ref. [12]. This revealed negative values for low temperatures, indicative of a diamagnetic response (due to pions). On the other hand, at high temperatures  $\chi^r$  is positive, revealing paramagnetism (due to quarks). In the electric case we have yet to perform the analytic continuation to obtain the susceptibility with respect to real electric fields.

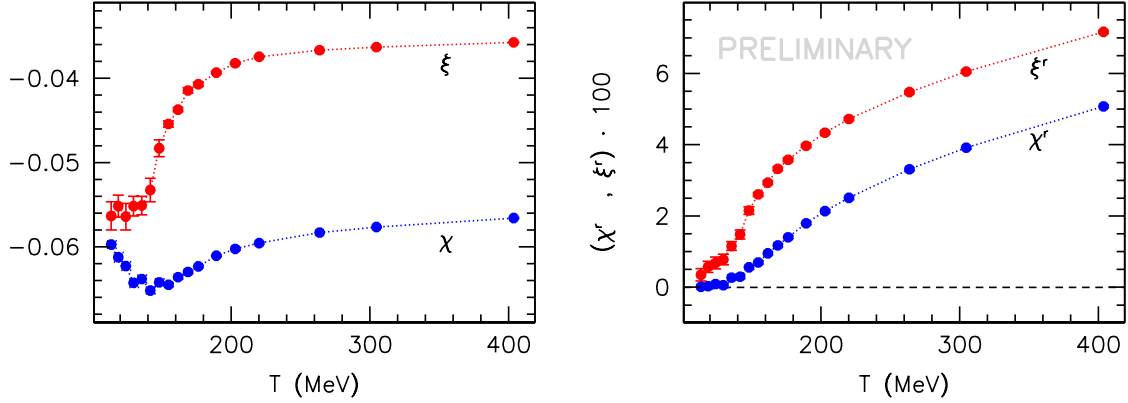


**Figure 4:** Bare (left panel) and renormalized (right panel) susceptibilities as a function of the temperature on  $24^3 \times 6$  lattices. Susceptibilities with respect to magnetic (blue) and imaginary electric (red) fields are both shown.

## 5. Summary

In this contribution we discussed the response of the thermal QCD medium to external electric fields, quantified in terms of the electric susceptibility. We demonstrated how to define the effect of the electric field by considering solely equilibrium simulations involving oscillatory field profiles. We also pointed out that at nonzero temperatures the electric field mixes with the chemical potential and contributes an infrared divergent term to the susceptibility. This divergence can be avoided if an averaging over the chemical potential variable at zero electric field is carried out. Finally we developed a Taylor-expansion scheme in the imaginary electric field, similarly to the recent approach for magnetic fields [12] and presented first results for the susceptibility.

**Acknowledgments** This research was funded by the DFG (Emmy Noether Programme EN 1064/2-1 and the Collaborative Research Center CRC-TR 211 “Strong-interaction matter under extreme conditions” – project number 315477589 - TRR 211).

## References

- [1] D. E. Kharzeev, K. Landsteiner, A. Schmitt, and H.-U. Yee, “‘Strongly interacting matter in magnetic fields’: an overview,” *Lect. Notes Phys.* **871** (2013) 1–11, [arXiv:1211.6245 \[hep-ph\]](#).
- [2] K. Tuchin, “Time and space dependence of electromagnetic field in relativistic heavy-ion collisions,” *Phys.Rev.* **C88** (2013) 024911, [arXiv:1305.5806 \[hep-ph\]](#).
- [3] L. McLerran and V. Skokov, “Comments About the Electromagnetic Field in Heavy-Ion Collisions,” [arXiv:1305.0774 \[hep-ph\]](#).
- [4] K. Fukushima, D. E. Kharzeev, and H. J. Warringa, “The Chiral Magnetic Effect,” *Phys. Rev.* **D78** (2008) 074033, [arXiv:0808.3382 \[hep-ph\]](#).

- [5] S. A. Voloshin, “Testing the Chiral Magnetic Effect with Central U+U collisions,” *Phys. Rev. Lett.* **105** (2010) 172301, [arXiv:1006.1020 \[nucl-th\]](#).
- [6] W.-T. Deng and X.-G. Huang, “Electric fields and chiral magnetic effect in Cu+Au collisions,” *Phys. Lett.* **B742** (2015) 296–302, [arXiv:1411.2733 \[nucl-th\]](#).
- [7] V. Voronyuk, V. D. Toneev, S. A. Voloshin, and W. Cassing, “Charge-dependent directed flow in asymmetric nuclear collisions,” *Phys. Rev.* **C90** no. 6, (2014) 064903, [arXiv:1410.1402 \[nucl-th\]](#).
- [8] M. D’Elia, S. Mukherjee, and F. Sanfilippo, “QCD Phase Transition in a Strong Magnetic Background,” *Phys. Rev.* **D82** (2010) 051501, [arXiv:1005.5365 \[hep-lat\]](#).
- [9] G. Bali, F. Bruckmann, G. Endrődi, Z. Fodor, S. Katz, *et al.*, “The QCD phase diagram for external magnetic fields,” *JHEP* **1202** (2012) 044, [arXiv:1111.4956 \[hep-lat\]](#).
- [10] G. Endrődi, “Critical point in the QCD phase diagram for extremely strong background magnetic fields,” *JHEP* **07** (2015) 173, [arXiv:1504.08280 \[hep-lat\]](#).
- [11] G. Bali, F. Bruckmann, G. Endrődi, S. Katz, and A. Schäfer, “The QCD equation of state in background magnetic fields,” *JHEP* **1408** (2014) 177, [arXiv:1406.0269 \[hep-lat\]](#).
- [12] G. S. Bali, G. Endrődi, and S. Piemonte, “Magnetic susceptibility of QCD matter and its decomposition from the lattice,” *JHEP* **07** (2020) 183, [arXiv:2004.08778 \[hep-lat\]](#).
- [13] LHPC Collaboration, M. Engelhardt, “Neutron electric polarizability from unquenched lattice QCD using the background field approach,” *Phys. Rev.* **D76** (2007) 114502, [arXiv:0706.3919 \[hep-lat\]](#).
- [14] M. Lujan, A. Alexandru, W. Freeman, and F. Lee, “Electric polarizability of neutral hadrons from dynamical lattice QCD ensembles,” *Phys. Rev.* **D89** no. 7, (2014) 074506, [arXiv:1402.3025 \[hep-lat\]](#).
- [15] A. Yamamoto, “Lattice QCD with strong external electric fields,” *Phys. Rev. Lett.* **110** no. 11, (2013) 112001, [arXiv:1210.8250 \[hep-lat\]](#).
- [16] H. Gies, “QED effective action at finite temperature,” *Phys. Rev. D* **60** (1999) 105002, [arXiv:hep-ph/9812436](#).
- [17] W. Detmold, B. C. Tiburzi, and A. Walker-Loud, “Extracting Electric Polarizabilities from Lattice QCD,” *Phys. Rev.* **D79** (2009) 094505, [arXiv:0904.1586 \[hep-lat\]](#).
- [18] G. ’t Hooft, “A Property of Electric and Magnetic Flux in Nonabelian Gauge Theories,” *Nucl. Phys.* **B153** (1979) 141–160.
- [19] G. Bali and G. Endrődi, “Hadronic vacuum polarization and muon  $g-2$  from magnetic susceptibilities on the lattice,” *Phys. Rev.* **D92** no. 5, (2015) 054506, [arXiv:1506.08638 \[hep-lat\]](#).



- [20] G. S. Bali, F. Bruckmann, G. Endrődi, and A. Schäfer, “Magnetization and pressures at nonzero magnetic fields in QCD,” *PoS LATTICE2013* (2014) 182, [arXiv:1310.8145 \[hep-lat\]](#).